# Design of Optimal Quincunx Filter Banks for Image Coding

Yi Chen, Michael D. Adams, and Wu-Sheng Lu
Dept. of Elec. and Comp. Engineering
University of Victoria, Victoria, BC, Canada

***Abstract*— A new technique is proposed for the design of high-performance quincunx filter banks for the application of image coding. This method yields linear-phase perfect-reconstruction systems with high coding gain, good analysis/synthesis filter frequency responses, and prescribed vanishing moment properties. Examples of filter banks designed with this technique are presented and shown to be highly effective for image coding.**

## I. Introduction

Filter banks have proven to be a highly effective tool for image coding applications [1]. Although techniques for the design of one-dimensional (1D) filter banks have become highly evolved, the nonseparable two-dimensional (2D) design case is much more difficult and far fewer effective methods have been proposed. In image coding applications, one typically desires filter banks with all of the following characteristics: perfect reconstruction (PR), linear phase, high coding gain [2], good frequency selectivity, and satisfactory vanishing moment properties. As it turns out, designing nonseparable 2D filter banks with all of the preceding properties is an extremely challenging task. In this paper, we propose a new optimization-based technique for constructing (nonseparable 2D) quincunx filter banks with all of the desirable characteristics mentioned above, where we formulate the design as a second-order cone programming (SOCP) problem [3] utilizing the lifting framework [4]. Although lifting-based design methods for quincunx filter banks have been proposed in [5], [6], these methods only consider the case of interpolating filter banks (i.e., filter banks with two lifting steps). Herein, we examine the more general case.

The remainder of this paper is structured as follows. Section II briefly introduces some notation and terminology used herein. Quincunx filter banks are then discussed in Section III, and our new design method is presented in Section IV. In Section V, we present some new filter banks obtained with our method and demonstrate their effectiveness for image coding. Finally, Section VI concludes with a summary of our work and some closing remarks.

## II. Notation and Terminology

In this paper, matrices and vectors are denoted by upper and lower case boldface letters, respectively. For matrix multiplication, we define the product notation as $\prod_{k=M}^{N} \boldsymbol{A}_k \triangleq \boldsymbol{A}_N \boldsymbol{A}_{N-1} \cdots \boldsymbol{A}_{M+1} \boldsymbol{A}_M$ for $N \geq M$. The sets of integers and ordered pairs of integers are denoted as $\mathbb{Z}$ and $\mathbb{Z}^2$, respectively. An element of a sequence $x$ defined on $\mathbb{Z}^2$ is denoted either as $x[\boldsymbol{n}]$ or $x[n_0, n_1]$ (whichever is more convenient), where $\boldsymbol{n} = [n_0 \;\; n_1]^T$ and $n_0, n_1 \in \mathbb{Z}$. Let $\boldsymbol{n} = [n_0 \;\; n_1]^T$, $\boldsymbol{z} = [z_0 \;\; z_1]^T$. Then, we define $|\boldsymbol{n}| = n_0 + n_1$ and $\boldsymbol{z}^{\boldsymbol{n}} = z_0^{n_0} z_1^{n_1}$. Furthermore, for a matrix $\boldsymbol{M} = [\boldsymbol{m}_0 \;\; \boldsymbol{m}_1]$ with $\boldsymbol{m}_k$ being the $k$th column of $\boldsymbol{M}$, we define $\boldsymbol{z}^{\boldsymbol{M}} = [\boldsymbol{z}^{\boldsymbol{m}_0} \;\; \boldsymbol{z}^{\boldsymbol{m}_1}]^T$. In what follows, unless otherwise noted, we will use $\boldsymbol{M}$ to denote the generating matrix $\left[\begin{smallmatrix} 1 & 1 \\ 1 & -1 \end{smallmatrix}\right]$ of the quincunx lattice.

The Fourier transform of a sequence $h$ is denoted as $\hat{h}$. A (2D) filter H with impulse response $h$ is said to be symmetric linear phase with group delay $\boldsymbol{c}$ if, for some $\boldsymbol{c} \in \frac{1}{2}\mathbb{Z}^2$, $h[\boldsymbol{n}] = h[2\boldsymbol{c} - \boldsymbol{n}]$ for all $\boldsymbol{n} \in \mathbb{Z}^2$. In passing, we note that the frequency response $\hat{h}(\boldsymbol{\omega})$ of a linear-phase filter with group delay $\boldsymbol{c}$ and impulse response $h$ can be expressed as

$$\hat{h}(\boldsymbol{\omega}) = e^{-j\boldsymbol{\omega}^T \boldsymbol{c}} \sum_{\boldsymbol{n} \in \mathbb{Z}^2} h[\boldsymbol{n}] \cos\left(\boldsymbol{\omega}^T (\boldsymbol{n} - \boldsymbol{c})\right). \tag{1}$$

This work was supported, in part, by the Natural Sciences and Engineering Research Council of Canada.

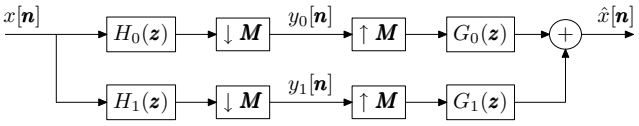


Fig. 1. Canonical form of a quincunx filter bank.

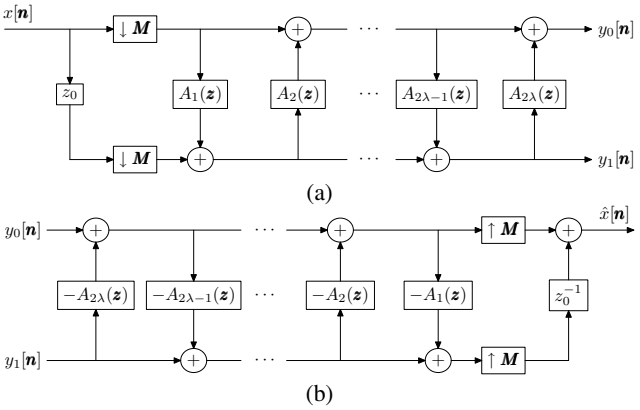


Fig. 2. Lifting realization of a quincunx filter bank. (a) Analysis side and (b) synthesis side.

## III. Quincunx Filter Banks

The canonical form of a quincunx filter bank is as shown in Fig. 1, and consists of lowpass and highpass analysis filters $\mathrm{H}_0$ and $\mathrm{H}_1$, lowpass and highpass synthesis filters $\mathrm{G}_0$ and $\mathrm{G}_1$, and $\boldsymbol{M}$-fold downsamplers and upsamplers. Rather than parameterizing the filter bank in terms of its canonical form, we instead employ the lifting framework [4]. The lifting realization of a quincunx filter bank has the form shown in Fig. 2. Essentially, the filter bank is realized in polyphase form, with the analysis and synthesis polyphase filtering each being performed by a ladder network consisting of $2\lambda$ lifting filters $\{\mathrm{A}_k\}$. Without loss of generality, we may assume that none of the $\{A_k(\boldsymbol{z})\}$ are identically zero, except possibly $A_1(\boldsymbol{z})$ and $A_{2\lambda}(\boldsymbol{z})$.

Given the lifting filters $\{\mathrm{A}_k\}$, the corresponding analysis filter transfer functions $H_0(\boldsymbol{z})$ and $H_1(\boldsymbol{z})$ can be calculated as

$$H_k(\boldsymbol{z}) = H_{k,0}\left(\boldsymbol{z}^{\boldsymbol{M}}\right) + z_0 H_{k,1}\left(\boldsymbol{z}^{\boldsymbol{M}}\right), \tag{2}$$

where $\begin{bmatrix} H_{0,0}(\boldsymbol{z}) & H_{0,1}(\boldsymbol{z}) \\ H_{1,0}(\boldsymbol{z}) & H_{1,1}(\boldsymbol{z}) \end{bmatrix} = \prod_{k=1}^{\lambda} \left( \begin{bmatrix} 1 & A_{2k}(\boldsymbol{z}) \\ 0 & 1 \end{bmatrix} \begin{bmatrix} 1 & 0 \\ A_{2k-1}(\boldsymbol{z}) & 1 \end{bmatrix} \right)$.

The synthesis filter transfer functions $G_0(\boldsymbol{z})$ and $G_1(\boldsymbol{z})$ can then be trivially computed as $G_k(\boldsymbol{z}) = (-1)^{1-k} z_0^{-1} H_{1-k}(-\boldsymbol{z})$.

The use of the above lifting-based parameterization is helpful in a number of regards. First, the PR condition is structurally imposed. Furthermore, we can structurally impose the linear-phase condition

with relative ease, as we shall see momentarily. This eliminates the need for additional cumbersome constraints (for PR and linear phase) during optimization. Lastly, we can trivially construct reversible integer-to-integer mappings from the lifting realization [7].

As was suggested above, it is possible to structurally impose the linear-phase condition with a prudent choice of lifting filters in Fig. 2. Suppose that the lifting filters $\{\mathrm{A}_k\}$ are symmetric, with the filter $\mathrm{A}_k$ having group delay $\boldsymbol{c}_k$. Then, the filter bank will have linear phase if each of the group delays satisfy

$$\boldsymbol{c}_k = (-1)^k \left[\begin{smallmatrix} \frac{1}{2} & \frac{1}{2} \end{smallmatrix}\right]^T. \tag{3}$$

In particular, with the preceding constraint on the choice of lifting filters, one can show that the analysis filters $\mathrm{H}_0$ and $\mathrm{H}_1$ will have linear phase with group delays $[0\ 0]^T$ and $[-1\ 0]^T$, respectively. (The proof is by induction, and is omitted here in the interest of brevity.)

In image coding applications, a quincunx filter bank is typically applied in a recursive manner, resulting in an octave-band filter bank structure. For an $N$-level octave-band filter bank generated from a quincunx filter bank with analysis filters $\{\mathrm{H}_k\}$, the equivalent nonuniform filter bank has $N+1$ channels with analysis filters $\{\mathrm{H}'_i\}$ and synthesis filters $\{\mathrm{G}'_i\}$. The transfer functions of the analysis filters $\{\mathrm{H}'_i\}$ are given by

$$H'_i(\boldsymbol{z}) = \begin{cases} \prod_{k=0}^{N-1} H_0\left(\boldsymbol{z}^{\boldsymbol{M}^k}\right) & i = 0 \\ H_1\left(\boldsymbol{z}^{\boldsymbol{M}^{N-i}}\right) \prod_{k=0}^{N-i-1} H_0\left(\boldsymbol{z}^{\boldsymbol{M}^k}\right) & 1 \le i \le N-1 \\ H_1(\boldsymbol{z}) & i = N. \end{cases} \tag{4}$$

The transfer functions of the synthesis filters $\{\mathrm{G}'_i\}$ can be derived in a similar fashion.

### A. Coding Gain

Coding gain is a measure of the energy compaction ability of a filter bank, and is defined as the ratio between the reconstruction error variance obtained by quantizing a signal directly to that obtained by quantizing the corresponding subband coefficients using an optimal bit allocation strategy. For an $N$-level octave-band filter bank, the coding gain $G_{SBC}$ can be computed as [2]

$$G_{SBC} = \prod_{k=0}^{N} (A_k B_k / \alpha_k)^{-\alpha_k}, \tag{5}$$

$$\text{where } A_k = \sum_{\boldsymbol{m}\in\mathbb{Z}^2} \sum_{\boldsymbol{n}\in\mathbb{Z}^2} h'_k[\boldsymbol{m}] h'_k[\boldsymbol{n}] r[\boldsymbol{m}-\boldsymbol{n}],\ B_k = \alpha_k \sum_{\boldsymbol{n}\in\mathbb{Z}^2} g'^2_k[\boldsymbol{n}],$$

$\alpha_0 = 2^{-N}$, $\alpha_k = 2^{-(N+1-k)}$ for $k = 1, 2, \ldots, N$, $h'_k[\boldsymbol{n}]$ and $g'_k[\boldsymbol{n}]$ are the impulse responses of the equivalent analysis and synthesis filters $\mathrm{H}'_k$ and $\mathrm{G}'_k$, and $r$ is the autocorrelation of the input. Depending on the source image model, $r$ is given by

$$r[n_0, n_1] = \begin{cases} \rho^{|n_0|+|n_1|} & \text{for separable model} \\ \rho^{\sqrt{n_0^2+n_1^2}} & \text{for isotropic model,} \end{cases} \tag{6}$$

where $\rho$ is the correlation coefficient (typically, $0.90 \le \rho \le 0.95$).

### B. Vanishing Moments

The number of vanishing moments is important in the design of filter banks, as it represents the ability to provide smooth image representations. It is equivalent to the order of zero at $[0\ 0]^T$ in the analysis or synthesis highpass-filter frequency response.

For a linear-phase filter H with group delay $\boldsymbol{c} \in \mathbb{Z}^2$, its Fourier transform $\hat{h}(\boldsymbol{\omega})$ can be computed by (1). The partial derivative of $\hat{h}(\boldsymbol{\omega})$ without the exponential factor is

$$\frac{\partial^{m_0+m_1} \hat{h}}{\partial \omega_0^{m_0} \partial \omega_1^{m_1}} = \begin{cases} \sum_{\boldsymbol{n}\in\mathbb{Z}^2} h[\boldsymbol{n}] (\boldsymbol{n}-\boldsymbol{c})^{\boldsymbol{m}} \cos\left(\boldsymbol{\omega}^T (\boldsymbol{n}-\boldsymbol{c})\right) & \text{for } |\boldsymbol{m}| \text{ even} \\ -\sum_{\boldsymbol{n}\in\mathbb{Z}^2} h[\boldsymbol{n}] (\boldsymbol{n}-\boldsymbol{c})^{\boldsymbol{m}} \sin\left(\boldsymbol{\omega}^T (\boldsymbol{n}-\boldsymbol{c})\right) & \text{otherwise,} \end{cases}$$

where $\boldsymbol{m} = [m_0\ m_1]^T$. To have an $N$th order zero at $\boldsymbol{\omega} = [0\ 0]^T$, the filter coefficients must satisfy

$$\sum_{\boldsymbol{n}\in\mathbb{Z}^2} h[\boldsymbol{n}] (\boldsymbol{n}-\boldsymbol{c})^{\boldsymbol{m}} = 0 \quad \text{for all even } |\boldsymbol{m}| \text{ such that } |\boldsymbol{m}| < N. \tag{7}$$

## IV. Optimal Design Algorithm

The design problem at hand will be formulated as an SOCP problem where a linear function is minimized subject to a set of second-order cone constraints [3]:

$$\begin{aligned} &\text{minimize} && \boldsymbol{b}^T \boldsymbol{x} \\ &\text{subject to:} && \|\boldsymbol{A}_i^T \boldsymbol{x} + \boldsymbol{c}_i\| \le \boldsymbol{b}_i^T \boldsymbol{x} + d_i \quad \text{for } i = 1, \ldots, q. \end{aligned} \tag{8}$$

### A. Filter Banks with Two Lifting Steps

Consider a filter bank constructed with the lifting structure as in Fig. 2. We begin with the simplest case with two lifting steps $\mathrm{A}_1$ and $\mathrm{A}_2$. In order for the analysis filters to have linear phase, $\mathrm{A}_1$ and $\mathrm{A}_2$ are both symmetric with group delays satisfying (3). Let $\boldsymbol{x} = [\boldsymbol{a}_1 \atop \boldsymbol{a}_2]$, where $\boldsymbol{a}_1$ and $\boldsymbol{a}_2$ contain the $n_1$ and $n_2$ independent coefficients of $\mathrm{A}_1$ and $\mathrm{A}_2$, respectively, and $\boldsymbol{x} \in \mathbb{R}^{n\times 1}$ with $n = n_1 + n_2$.

*1) Vanishing Moments:* In order for the filter bank to have $N_p$ primal and $N_d$ dual vanishing moments, $\boldsymbol{x}$ needs to be the solution of an underdetermined linear system [6]

$$\boldsymbol{A}\boldsymbol{x} = \boldsymbol{b}, \tag{9}$$

where $\boldsymbol{A} \in \mathbb{R}^{m\times n}$ with rank $r$, $\boldsymbol{b} \in \mathbb{R}^{m\times 1}$ and $m < n$. By computing the singular value decomposition (SVD) of $\boldsymbol{A} = \boldsymbol{U}\boldsymbol{S}\boldsymbol{V}^T$, the solutions to (9) can be parameterized as

$$\boldsymbol{x} = \underbrace{\boldsymbol{A}^+ \boldsymbol{b}}_{\boldsymbol{x}_s} + \boldsymbol{V}_r \boldsymbol{\phi} = \boldsymbol{x}_s + \boldsymbol{V}_r \boldsymbol{\phi}, \tag{10}$$

where $\boldsymbol{A}^+$ is the Moore-Penrose pseudoinverse of $\boldsymbol{A}$, $\boldsymbol{V}_r$ is a matrix composed of the last $n-r$ columns of $\boldsymbol{V}$, and $\boldsymbol{\phi}$ is an arbitrary vector with $n-r$ elements. In what follows, we use $\boldsymbol{\phi}$ as the design vector. Thus, the number of parameters involved is reduced from $n$ to $n-r$.

*2) Coding Gain:* Combining equations (2), (4), (5), (6) and (10), the coding gain $G_{SBC}$ of an $N$-level octave-band filter bank can be written as a nonlinear function of $\boldsymbol{\phi}$. By taking the logarithm $G = -10\log_{10} G_{SBC}$, the problem of maximizing $G_{SBC}$ is equivalent to minimizing $G$. Our design strategy is that, for a given parameter vector $\boldsymbol{\phi}$, we seek a small perturbation $\boldsymbol{\delta}_{\boldsymbol{\phi}}$ such that $G(\boldsymbol{\phi} + \boldsymbol{\delta}_{\boldsymbol{\phi}})$ is reduced relative to $G(\boldsymbol{\phi})$. Because $\|\boldsymbol{\delta}_{\boldsymbol{\phi}}\|$ is small, we can write the quadratic and linear approximations of $G(\boldsymbol{\phi} + \boldsymbol{\delta}_{\boldsymbol{\phi}})$ as

$$G(\boldsymbol{\phi} + \boldsymbol{\delta}_{\boldsymbol{\phi}}) \approx G(\boldsymbol{\phi}) + \boldsymbol{g}^T \boldsymbol{\delta}_{\boldsymbol{\phi}} + \frac{1}{2} \boldsymbol{\delta}_{\boldsymbol{\phi}}^T \boldsymbol{Q} \boldsymbol{\delta}_{\boldsymbol{\phi}} \quad \text{and} \tag{11}$$

$$G(\boldsymbol{\phi} + \boldsymbol{\delta}_{\boldsymbol{\phi}}) \approx G(\boldsymbol{\phi}) + \boldsymbol{g}^T \boldsymbol{\delta}_{\boldsymbol{\phi}}, \tag{12}$$

respectively, where $\boldsymbol{g}$ is the gradient and $\boldsymbol{Q}$ is the Hessian at point $\boldsymbol{\phi}$. Having obtained such a $\boldsymbol{\delta}_{\boldsymbol{\phi}}$ (subject to some additional constraint to be described shortly), the parameter vector $\boldsymbol{\phi}$ is updated to $\boldsymbol{\phi} + \boldsymbol{\delta}_{\boldsymbol{\phi}}$. This iterative process continues until the reduction $\left|G(\boldsymbol{\phi} + \boldsymbol{\delta}_{\boldsymbol{\phi}}) - G(\boldsymbol{\phi})\right|$ becomes less than a prescribed tolerance $\varepsilon$.

*3) Frequency Response:* The constraint on frequency selectivity can be formulated as a second-order cone. We define the weighted error function of the frequency response of highpass analysis filter $\mathrm{H}_1$ as

$$e_{h_1} = \int_{[-\pi,\,\pi)^2} W(\boldsymbol{\omega}) \left|\hat{h}_1(\boldsymbol{\omega}) - \hat{h}_{ideal}(\boldsymbol{\omega})\right|^2 \mathrm{d}\boldsymbol{\omega}, \tag{13}$$

where $W(\boldsymbol{\omega})$ is a weighting function with different weights for the stopband, transition band and passband, and $\hat{h}_{ideal}(\boldsymbol{\omega})$ is the ideal frequency response for a quincunx highpass filter. In order for the filter $\mathrm{H}_1$ to have good frequency response, $e_{h_1}$ is required to satisfy

$$e_{h_1} \le \delta_{h_1}, \tag{14}$$

where $\delta_{h_1}$ is a prescribed upper bound for the error function. From (2), the Fourier transform of $H_1$ can be written as

$$\hat{h}_1(\boldsymbol{\omega}) = \hat{a}_1(\boldsymbol{M}^T\boldsymbol{\omega}) + e^{j\omega_0}. \tag{15}$$

Since $A_1$ has linear-phase, $\hat{a}_1(\boldsymbol{\omega})$ assumes the form in (1). Thus, $\hat{a}_1(\boldsymbol{M}^T\boldsymbol{\omega})$ can be written as

$$\hat{a}_1(\boldsymbol{M}^T\boldsymbol{\omega}) = e^{j\omega_0}\boldsymbol{a}_1^T\boldsymbol{v}_1(\boldsymbol{\omega}), \tag{16}$$

where $\boldsymbol{a}_1$ is the vector of independent coefficients of $A_1$, and $v_1(\boldsymbol{\omega})$ is a vector of cosine functions of $\boldsymbol{\omega}$. The vector $\boldsymbol{a}_1$ can be expressed in terms of $\boldsymbol{\phi}$ by

$$\boldsymbol{a}_1 = \underbrace{[\boldsymbol{I}_{n_1} \quad \boldsymbol{0}]}_{\tilde{\boldsymbol{I}}}\boldsymbol{x} = \tilde{\boldsymbol{I}}(\boldsymbol{x}_s + \boldsymbol{V}_r\boldsymbol{\phi}) = \underbrace{\tilde{\boldsymbol{I}}\boldsymbol{x}_s}_{\tilde{\boldsymbol{x}}_s} + \underbrace{\tilde{\boldsymbol{I}}\boldsymbol{V}_r}_{\tilde{\boldsymbol{V}}_r}\boldsymbol{\phi} = \tilde{\boldsymbol{x}}_s + \tilde{\boldsymbol{V}}_r\boldsymbol{\phi}, \tag{17}$$

where $\boldsymbol{I}_{n_1}$ is an identity matrix of size $n_1 \times n_1$.

From (13), (15), (16) and (17), $e_{h_1}$ can be viewed as a quadratic function of $\boldsymbol{\phi}$ given by

$$e_{h_1} = \boldsymbol{\phi}^T\boldsymbol{H}_{\boldsymbol{\phi}}\boldsymbol{\phi} + \boldsymbol{\phi}^T\boldsymbol{s}_{\boldsymbol{\phi}} + C_{\boldsymbol{\phi}}, \tag{18}$$

where $\boldsymbol{H}_{\boldsymbol{\phi}}$ is a symmetric positive semidefinite matrix, $\boldsymbol{s}_{\boldsymbol{\phi}}$ is a vector, and $C_{\boldsymbol{\phi}}$ is a constant. If we replace $\boldsymbol{\phi}$ by $\boldsymbol{\phi} + \boldsymbol{\delta}_{\boldsymbol{\phi}}$ and let the SVD of $\boldsymbol{H}_{\boldsymbol{\phi}}$ be $\boldsymbol{U}_H\boldsymbol{\Sigma}\boldsymbol{V}_H^T$, then (18) can also be written as $e_{h_1} = \|\tilde{\boldsymbol{H}}\boldsymbol{\delta}_{\boldsymbol{\phi}} + \tilde{\boldsymbol{s}}\|^2 + \tilde{C}$, and the constraint (14) becomes a second-order cone

$$\|\tilde{\boldsymbol{H}}\boldsymbol{\delta}_{\boldsymbol{\phi}} + \tilde{\boldsymbol{s}}\|^2 \le \delta_{h_1} - \tilde{C}, \tag{19}$$

where $\tilde{\boldsymbol{H}} = \boldsymbol{\Sigma}^{\frac{1}{2}}\boldsymbol{U}_H^T$, $\tilde{\boldsymbol{s}} = \frac{1}{2}\tilde{\boldsymbol{H}}^{-T}\left(2\boldsymbol{H}_{\boldsymbol{\phi}}\boldsymbol{\phi} + \boldsymbol{s}_{\boldsymbol{\phi}}\right)$, and $\tilde{C} = \boldsymbol{\phi}^T\boldsymbol{H}_{\boldsymbol{\phi}}\boldsymbol{\phi} + \boldsymbol{\phi}^T\boldsymbol{s}_{\boldsymbol{\phi}} + C_{\boldsymbol{\phi}} - \|\tilde{\boldsymbol{s}}\|^2$.

*4) Design Algorithm:* Now we show how to employ the SOCP algorithm to solve the problem of maximizing the coding gain $G_{SBC}(\boldsymbol{x})$ with constraints $\boldsymbol{A}\boldsymbol{x} = \boldsymbol{b}$ as in (9) and $e_{h_1} \le \delta_{h_1}$ as in (14). This problem can be formulated as follows.

**Step 1** Compute $\boldsymbol{A}$ and $\boldsymbol{b}$ in (9) for the desired numbers of vanishing moments, and calculate $\boldsymbol{H}_{\boldsymbol{\phi}}$, $\boldsymbol{s}_{\boldsymbol{\phi}}$, and $C_{\boldsymbol{\phi}}$ in (18). Then, select an initial point $\boldsymbol{\phi}_0$.

**Step 2** For the $k$th iteration, at the point $\boldsymbol{\phi}_k$, compute the gradient $\boldsymbol{g}$ in (12) and $\tilde{\boldsymbol{H}}$, $\tilde{\boldsymbol{s}}$, and $\tilde{C}$ in (19), then solve the SOCP problem

$$\begin{aligned} \text{minimize} \quad & \boldsymbol{g}^T\boldsymbol{\delta}_{\boldsymbol{\phi}} \\ \text{subject to:} \quad & \|\tilde{\boldsymbol{H}}\boldsymbol{\delta}_{\boldsymbol{\phi}} + \tilde{\boldsymbol{s}}\| \le \sqrt{\delta_{h_1} - \tilde{C}} \\ & \|\boldsymbol{\delta}_{\boldsymbol{\phi}}\| \le \beta, \end{aligned} \tag{20}$$

where $\beta$ is a given small value used to ensure that the solution is within the vicinity of $\boldsymbol{\phi}_k$. More details about the choice of $\beta$ and $\delta_{h_1}$ in (20) can be found in [8]. We use the SeDuMi optimization package [9] to seek the optimal solution $\boldsymbol{\delta}_{\boldsymbol{\phi}}$, and then update $\boldsymbol{\phi}_k$ to $\boldsymbol{\phi}_{k+1} = \boldsymbol{\phi}_k + \boldsymbol{\delta}_{\boldsymbol{\phi}}$.

**Step 3** If $|G(\boldsymbol{\phi}_{k+1}) - G(\boldsymbol{\phi}_k)| < \varepsilon$, then output $\boldsymbol{\phi}^* = \boldsymbol{\phi}_{k+1}$, compute $\boldsymbol{x}^* = \boldsymbol{x}_s + \boldsymbol{V}_r\boldsymbol{\phi}^*$, and stop. Otherwise, go to step 2.

The vector $\boldsymbol{x}^*$ is then the optimal solution to this problem. The filter bank constructed with the lifting filter coefficients in $\boldsymbol{x}^*$ has high coding gain, good frequency responses, and the desired number of vanishing moments. We can also use the quadratic approximation of $G(\boldsymbol{\phi} + \boldsymbol{\delta}_{\boldsymbol{\phi}})$ as in (11) in the design algorithm to improve the approximation accuracy.

### *B. Filter Banks with More Than Two Lifting Steps*

Consider a linear-phase quincunx filter bank constructed with $M$ lifting filters $A_1$, $A_2$, …, $A_M$ as in Fig. 2. Let $\boldsymbol{x}$ be the design vector consisting of $\boldsymbol{a}_1, \boldsymbol{a}_2, \ldots, \boldsymbol{a}_M$, where $\boldsymbol{a}_i$ contains the independent coefficients of filter $A_i$. In what follows, we show how to design such quincunx filter banks with all of the desirable properties identified earlier.

*1) Coding Gain:* The coding gain $G_{SBC}(\boldsymbol{x})$ of an $N$-level octave-band filter bank is computed by (5). The linear approximation of $G$ with $G(\boldsymbol{x}) = -10\log_{10}G_{SBC}(\boldsymbol{x})$ is given by

$$G(\boldsymbol{x} + \boldsymbol{\delta}_{\boldsymbol{x}}) = G(\boldsymbol{x}) + \boldsymbol{g}^T\boldsymbol{\delta}_{\boldsymbol{x}}, \tag{21}$$

where $\boldsymbol{g}$ is the gradient at point $\boldsymbol{x}$. Similar to the previous case, we iteratively seek a small perturbation $\boldsymbol{\delta}_{\boldsymbol{x}}$ such that $G(\boldsymbol{x} + \boldsymbol{\delta}_{\boldsymbol{x}})$ is reduced relative to $G(\boldsymbol{x})$ until the reduction is less than a prescribed tolerance.

*2) Vanishing Moments:* Using (7), we can write the constraint on the number of vanishing moments as a set of polynomial equations in $\boldsymbol{x}$. By substituting $\boldsymbol{x}$ by $\boldsymbol{x}_k + \boldsymbol{\delta}_{\boldsymbol{x}}$ with $\|\boldsymbol{\delta}_{\boldsymbol{x}}\|$ being small, these polynomial equations can be approximated by an underdetermined linear system

$$\boldsymbol{A}_k\boldsymbol{\delta}_{\boldsymbol{x}} = \boldsymbol{b}_k. \tag{22}$$

In this case, the filter bank constructed with lifting filter coefficients $\boldsymbol{x}_k + \boldsymbol{\delta}_{\boldsymbol{x}}$ has the desired number of approximate vanishing moments. The moments are typically extremely close to zero, as will be illustrated in Section V.

*3) Frequency Response:* We define the weighted error function $e_{h_1}$ of $\hat{h}_1(\boldsymbol{\omega})$ as in (13), and $e_{h_1}$ must satisfy the constraint (14). From (2), we know that $\hat{h}_1(\boldsymbol{\omega})$ is a polynomial in $\boldsymbol{x}$ of order no less than two. Similarly, we replace $\boldsymbol{x}$ by $\boldsymbol{x}_k + \boldsymbol{\delta}_{\boldsymbol{x}}$. If $\|\boldsymbol{\delta}_{\boldsymbol{x}}\|$ is small enough, we can omit the second and higher order terms of $\boldsymbol{\delta}_{\boldsymbol{x}}$ in $\hat{h}_1(\boldsymbol{\omega})$, and a quadratic approximation of $e_{h_1}$ is obtained as

$$e_{h_1} = \boldsymbol{\delta}_{\boldsymbol{x}}^T\boldsymbol{H}_k\boldsymbol{\delta}_{\boldsymbol{x}} + \boldsymbol{\delta}_{\boldsymbol{x}}^T\boldsymbol{s}_k + C_k,$$

where $\boldsymbol{H}_k$ is a symmetric positive semidefinite matrix, and $\boldsymbol{H}_k$, $\boldsymbol{s}_k$ and $C_k$ are dependent on $\boldsymbol{x}_k$. Then, the constraint $e_{h_1} \le \delta_{h_1}$ can be expressed in the form of a second-order cone

$$\|\tilde{\boldsymbol{H}}_k\boldsymbol{\delta}_{\boldsymbol{x}} + \tilde{\boldsymbol{s}}_k\|^2 \le \delta_{h_1} - \tilde{C}_k. \tag{23}$$

*4) Design Algorithm:* We use an algorithm similar to that of the previous case to solve this design problem.

**Step 1** Select an initial point $\boldsymbol{x}_0$.

**Step 2** For the $k$th iteration, at the point $\boldsymbol{x}_k$, compute the gradient $\boldsymbol{g}$ of $G(\boldsymbol{x})$ in (21), $\boldsymbol{A}_k$ and $\boldsymbol{b}_k$ in (22) and $\tilde{\boldsymbol{H}}_k$, $\tilde{\boldsymbol{s}}_k$, and $\tilde{C}_k$ in (23), then solve the SOCP problem

$$\begin{aligned} \text{minimize} \quad & \boldsymbol{g}^T\boldsymbol{\delta}_{\boldsymbol{x}} \\ \text{subject to:} \quad & \boldsymbol{A}_k\boldsymbol{\delta}_{\boldsymbol{x}} = \boldsymbol{b}_k \\ & \|\tilde{\boldsymbol{H}}_k\boldsymbol{\delta}_{\boldsymbol{x}} + \tilde{\boldsymbol{s}}_k\| \le \sqrt{\delta_{h_1} - \tilde{C}_k} \\ & \|\boldsymbol{\delta}_{\boldsymbol{x}}\| \le \beta, \end{aligned}$$

where the linear constraint $\boldsymbol{A}_k\boldsymbol{\delta}_{\boldsymbol{x}} = \boldsymbol{b}_k$ can be parameterized as in the previous algorithm to reduce the number of design variables, or be approximated by $\|\boldsymbol{A}_k\boldsymbol{\delta}_{\boldsymbol{x}} - \boldsymbol{b}_k\| \le \varepsilon_\delta$ with $\varepsilon_\delta$ being a prescribed tolerance. Then, use the optimal solution $\boldsymbol{\delta}_{\boldsymbol{x}}$ to update $\boldsymbol{x}_k$ to $\boldsymbol{x}_{k+1} = \boldsymbol{x}_k + \boldsymbol{\delta}_{\boldsymbol{x}}$.

**Step 3** If $|G(\boldsymbol{x}_{k+1}) - G(\boldsymbol{x}_k)| < \varepsilon$, then output $\boldsymbol{x}^* = \boldsymbol{x}_{k+1}$ and stop. Otherwise, go to step 2.

## V. Design Examples

In order to demonstrate the effectiveness of our proposed design method, we now give two examples of filter banks constructed using our method. We then demonstrate their effectiveness for image coding.

Our first design, which will be henceforth referred to as CAL1, has two primal and two dual vanishing moments, and employs two lifting steps, each having a diamond support of $6 \times 6$. We optimized for maximal coding gain assuming an isotropic image model (with $\rho = 0.95$) and a six-level decomposition. The resulting filter bank has a coding gain of 12.06 dB, and lowpass analysis and synthesis filters

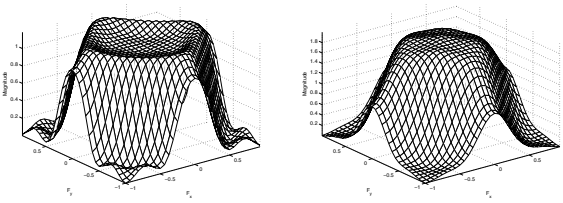

(a) (b)

Fig. 3. Filter frequency responses for CAL1 filter bank. Frequency responses of lowpass (a) analysis and (b) synthesis filters.

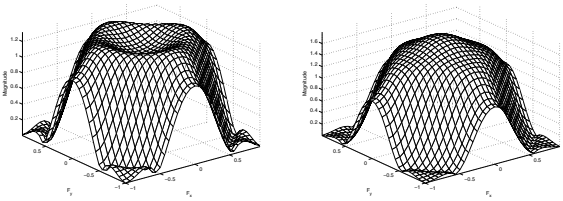

(a) (b)

Fig. 4. Filter frequency responses for CAL2 filter bank. Frequency responses of lowpass (a) analysis and (b) synthesis filters.

with the frequency responses shown in Fig. 3. (The highpass filter frequency responses are not given here, as they are simply modulated versions of lowpass filter frequency responses.)

Our second design, which will be henceforth referred to as CAL2, has two primal and two dual (approximate) vanishing moments, and employs three lifting steps, each having a diamond support of $4 \times 4$. Again, we optimized for maximal coding gain assuming an isotropic image model (with $\rho = 0.95$) and a six-level decomposition. The resulting filter bank has a coding gain of 12.23 dB, and lowpass filters with the frequency responses shown in Fig. 4. Although, strictly speaking, the moments are only near vanishing in this case, they are on the order of $10^{-12}$ to $10^{-17}$, which is small enough to be considered as zero for all practical purposes.

In what follows, for comparison purposes, we consider two filter banks produced by methods previously proposed by others. The first is a quincunx filter bank with six primal and six dual vanishing moments, constructed using the method of [6], and henceforth referred to by the name KS. The second is the well-known separable 9/7 filter bank [1], with four primal and four dual vanishing moments.

Table I provides the coding gains for our CAL1 and CAL2 designs as well as the KS and 9/7 filter banks. Clearly, the CAL1 and CAL2 designs have a larger coding gain than the quincunx KS filter bank. Furthermore, the CAL2 design also has a higher coding gain than the 9/7 filter bank, which is quite impressive considering that the 9/7 filter bank is well known for its high coding gain.

In order to further demonstrate the utility of our new filter banks, they were employed in a slightly modified version of the embedded lossy/lossless image coder developed by the second author of this paper [10]. This coder can be used with either nonseparable or separable filter banks based on the lifting framework (as is the case here). Reversible integer-to-integer versions of filter banks are employed. For the most part, the JPEG-2000 test images [11] were used in our experiments. Since our filter banks were designed for images that are more isotropic in nature, we have chosen to present coding results for such an image, namely the `finger` (i.e., fingerprint) image.

The `finger` image was coded in a lossy manner at various bit rates, using each of the CAL1, CAL2, KS, and 9/7 filter banks, and the resulting reconstruction errors measured. Six and three levels of decomposition were employed in the cases of the quincunx and separable filter banks, respectively. The results are shown in Table II. Clearly, both of the CAL2 and CAL1 filter banks perform very well, consistently outperforming the KS filter bank. The CAL2 design is even able to outperform the 9/7 filter bank, except at the lowest bit rate. This is a very encouraging result, as the 9/7 filter bank is generally held to be one of the very best in the literature. Lastly, it is worth noting that, although we only present results for the `finger` image herein, the CAL2 and CAL1 filter banks consistently outperform the KS filter bank for other images in the vast majority of cases.

TABLE I
CODING GAIN COMPARISON

| Transform | $G_{SBC}{}^{\dagger}$ (dB) |
|---|---|
| CAL1 | 12.06 |
| CAL2 | 12.23 |
| KS | 11.94 |
| 9/7 | 12.17 |

$^{\dagger}$coding gain

TABLE II
LOSSY COMPRESSION RESULTS FOR THE FINGER IMAGE

| CR$^{\dagger}$ | PSNR (dB) | | | |
|---|---|---|---|---|
| | CAL1 | CAL2 | KS | 9/7 |
| 128 | 19.88 | 19.95 | 19.67 | **19.98** |
| 64 | 21.70 | **21.75** | 21.53 | 21.72 |
| 32 | **24.52** | 24.39 | 24.36 | 24.20 |
| 16 | 27.75 | **27.83** | 27.65 | 27.61 |

$^{\dagger}$compression ratio

## VI. CONCLUSIONS

In this paper, we have proposed a new optimization-based method for the design of high-performance quincunx filter banks for the application of image coding. This method yields linear-phase PR systems with high coding gain, good analysis/synthesis filter frequency responses, and prescribed vanishing moment properties. Two examples of filter banks constructed with our method were presented and shown to work very well for image coding, thus demonstrating the effectiveness of our technique.

## REFERENCES


[1] *ISO/IEC 15444-1: Information technology—JPEG 2000 image coding system—Part 1: Core coding system*, 2000.

[2] J. Katto and Y. Yasuda, "Performance evaluation of subband coding and optimization of its filter coefficients," in *SPIE VCIP*, vol. 1605, Nov. 1991, pp. 95–106.

[3] M. S. Lobo, L. Vandenberghe, S. Boyd, and H. Lebret, "Applications of second-order cone programming," *Linear Algebra and Applications*, vol. 284, pp. 193–228, Nov. 1998.

[4] W. Sweldens, "The lifting scheme: A custom-design construction of biorthogonal wavelets," *Applied and Computational Harmonic Analysis*, vol. 3, pp. 186–200, 1996.

[5] S. M. Phoong, C. W. Kim, P. P. Vaidyanathan, and R. Ansari, "A new class of two-channel biorthogonal filter banks and wavelet bases," *IEEE Trans. on Signal Processing*, vol. 43, no. 3, pp. 649–665, Mar. 1995.

[6] J. Kovačević and W. Sweldens, "Wavelet families of increasing order in arbitrary dimensions," *IEEE Trans. on Image Processing*, vol. 9, pp. 480–496, Mar. 2000.

[7] A. R. Calderbank, I. Daubechies, W. Sweldens, and B.-L. Yeo, "Wavelet transforms that map integers to integers," *Applied and Computational Harmonic Analysis*, vol. 5, no. 3, pp. 332–369, July 1998.

[8] Y. Chen, "Design and application of quincunx filter banks," M.A.Sc. thesis, Dept. of Electrical and Computing Engineering, University of Victoria, Victoria, BC, Canada, 2006.

[9] J. Sturm, "Using SeDuMi 1.02, a MATLAB toolbox for optimization over symmetric cones," *Optimization Methods and Software*, vol. 11–12, pp. 625–653, 1999.

[10] M. D. Adams, "ELEC 545 project: A wavelet-based lossy/lossless image compression system," Dept. of Electrical and Computer Engineering, University of British Columbia, Vancouver, BC, Canada, Apr. 1999.

[11] "JPEG-2000 test images," ISO/IEC JTC 1/SC 29/WG 1 N 545, July 1997.